HTML ABSTRACT + LINKS

APPLIED PHYSICS LETTERS **86**, 202905 (2005)

The influence of an extrinsic interfacial layer on the polarization of sputtered $BaTiO_3$ film

Y. W. Cho, S. K. Choi,[a] and G. Venkata Rao
Department of Materials Science and Engineering, Korea Advanced Institute of Science and Technology, 373-1, Guseong-dong Yuseong-gu, Daejeon 305-701 Republic of Korea

(Received 26 July 2004; accepted 15 March 2005; published online 10 May 2005)

As an origin of degradation of remnant polarization in $Pt/BaTiO_3/Pt$ capacitor structure, an interfacial layer formed at the interface of $BaTiO_3$ film and a Pt bottom electrode is considered. $BaTiO_3$ films were deposited on two types of bottom electrodes ($La_{0.5}Sr_{0.5}CoO_3$ and Pt) by the radio frequency magnetron sputtering method and both capacitors showed a microstructural similarity with strong preferred orientations. However, a $Pt/BaTiO_3/La_{0.5}Sr_{0.5}CoO_3$ capacitor exhibited a saturated hysteresis loop with the remnant polarization ($2P_r$) of 6 $\mu C/cm^2$, and for the $Pt/BaTiO_3/Pt$ structure, the polarization-voltage curve revealed a linear dielectric characteristic. From a cross-sectional high-resolution transmission electron microscope analysis of the $Pt/BaTiO_3/Pt$ capacitor showing the linear dielectric property, an interfacial layer with an amorphous structure as well as a multidomain structure in the interior of the $BaTiO_3$ film were observed. It is concluded that the interfacial layer might help degradation of polarization and its origin can be classified as being extrinsic. © *2005 American Institute of Physics*.
[DOI: 10.1063/1.1921358]

The dielectric constant and polarization of ferroelectric film significantly reduces as its thickness decreases. This size effect of ferroelectric film can be understood by assuming the existence of an interfacial layer with a low dielectric constant at an electrode–ferroelectric interface.[1–5] The equivalent circuit of a ferroelectric capacitor with this layer is represented by a series capacitance model comprising two interfacial capacitances (C_i) and a bulk capacitance (C_f). The measured apparent capacitance (C_m) at zero field can therefore be expressed as

$$A/C_m = A/C_i + A/C_f = d_i/\varepsilon_i + (d_m - d_i)/\varepsilon_f = d_m/\varepsilon_m, \qquad (1)$$

where A is the electrode area, ε_f is the bulk dielectric constant of the film, ε_i is the interfacial layer dielectric constant, ε_m is the measured dielectric constant, d_m is the total film thickness, and d_i is interfacial layer thickness. The d_i/ε_i of the interfacial layer can be obtained from the y axis-intercept of the variations of d_m/ε_m as a function of film thickness.

Recently, Streiffer *et al.*[2] classified the origins of the interfacial layer into intrinsic and extrinsic phenomena. Intrinsic causes consist of incomplete polarization screening by the conducting electrode, interfacial discontinuity effects, and electrode-film band offsets. Extrinsic causes include the contamination of the film–electrode interfaces and a change in composition or grain size in the near-interface region. However, the nature of the interfacial layer is still disputed because the measured interfacial capacitance is likely to include intrinsic and extrinsic phenomena. Exact knowledge of the space charge distribution (depleted or accumulated mode) of ferroelectric capacitor structures is also required to identify the features of the intrinsic interfacial layer.[6,7] Furthermore, few experimental results have been published that directly show the existence of the interfacial layer through transmission electron microscopy (TEM) analysis. In this study, we find evidence of an extrinsic interfacial layer formed at the interface of $BaTiO_3$ film and a Pt bottom electrode through high resolution TEM (HRTEM) images and suggest this as the possible cause of polarization degradation.

The $BaTiO_3$ films were deposited on a $LSCO/LaAlO_3$ and $Pt/Ti/SiO_2/Si$ substrate by radio frequency (rf) magnetron sputtering using a polycrystalline $BaTiO_3$ ceramic target with a diameter of 2 in. Additionally, $BaTiO_3$ film with thickness ranging from 60 to 280 nm was deposited on the $Pt/Ti/SiO_2/Si$ substrate to obtain information on d_i/ε_i of the interfacial layer. Highly (100)-oriented LSCO film with a thickness of 200 nm was deposited on a $LaAlO_3$ substrate by direct current (dc) magnetron sputtering. Details of the LSCO film preparation are described elsewhere.[8] The sputtering atmosphere was pure argon (99.99%) under a working pressure of 10 mTorr. The $BaTiO_3$ film, which was deposited at a substrate temperature of 400 °C under 120 W rf power, was directly inserted into a preheated furnace at 750 °C in air for 2 h. The wavelength dispersive x-ray spectroscopy (WDS) clarified that this heat treatment maintained the Ba/Ti ratio of all $BaTiO_3$ films on both electrodes (LSCO and Pt) at nearly 1:1. The top electrodes of the Pt (100 nm), with a diameter of 0.4 mm, were deposited by dc magnetron sputtering to form the ferroelectric capacitors.

Figure 1(a) shows that the 100 nm thick $BaTiO_3$ film grown on LSCO-coated $LaAlO_3$ exhibits a (00*l*) preferred orientation. However, from the (00*l*) peaks, it cannot be determined whether the $BaTiO_3$ film consists of either (100)- or (001)-preferred orientation or a mixture of (100)- and (001)-

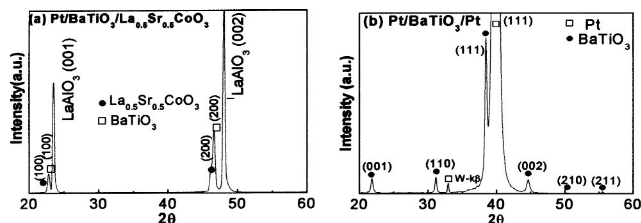

FIG. 1. X-ray diffraction patterns of $BaTiO_3$ film on $La_{0.5}Sr_{0.5}CoO_3/LaAlO_3$ (a) and $Pt/Ti/SiO_2/Si$ (b) after postannealing.

[a]Electronic mail: sikchoi50@kaist.ac.kr

Downloaded 18 Apr 2011 to 143.248.103.56. Redistribution subject to AIP license or copyright; see http://apl.aip.org/about/rights_and_permissions

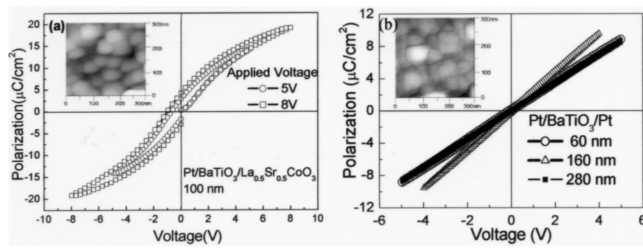

FIG. 2. $P-V$ hysteresis loops for (a) $Pt/BaTiO_3/La_{0.5}Sr_{0.5}CoO_3/LaAlO_3$ capacitor with a thickness of 100 nm and (b) $Pt/BaTiO_3/Pt/Ti/SiO_2/Si$ capacitor with various film thicknesses. (Note that the curve of 60 nm overlapped with that of 280 nm.) Scanning probe microscopy surface topographic images of $BaTiO_3$ film with a thickness of 100 nm, presented in the insets of the figure, clearly show that both types of capacitor have the same grain size of 50 nm.

preferred orientation. On the other hand, the $BaTiO_3$ film on $Pt/Ti/SiO_2/Si$ in Fig. 2(b) shows a strong (111)-preferred orientation, which corresponds well with the bottom electrode having Pt (111) orientation. Note that the $BaTiO_3$ films with a preferred orientation have a columnar structure since their surface morphology reveals polycrystal structure (the insets of Fig. 2). In this work, the ferroelectric films deposited at a low temperature (400 °C) were postannealed at a high temperature (750 °C) for 2 h. The crystallization of the film could therefore be completed through crystal nucleation and growth. The final orientation of the film grains reportedly depends on the orientations of the initial nuclei.[9,10]

Figure 2 shows the $P-V$ hysteresis loops of $BaTiO_3$ thin films deposited on LSCO and a Pt electrode. As shown in Fig. 2(a), the remnant polarization ($2P_r$) and the coercive field (E_c) for the $BaTiO_3$ film grown on an LSCO electrode is 6 $\mu C/cm^2$ and 1 V, respectively; the $BaTiO_3$ film on the LSCO electrode clearly shows ferroelectricity. However, the $P-V$ measurements for the $BaTiO_3/Pt/Ti/SiO_2/Si$ structures with various film thicknesses indicate typical linear dielectric characteristics, as shown in Fig. 2(b); $BaTiO_3$ films on the Pt electrode clearly lose ferroelectricity. Although all $BaTiO_3$ films on both electrodes have the same Ba/Ti ratio, the complete loss of ferroelectricity in the $BaTiO_3$ films on the Pt electrode is very interesting.

The reduction in film thickness that accompanies the decrease of grain size can degrade the remnant polarization in ABO_3-type ferroelectric films.[11,12] The scanning probe microscopy surface topographic images presented in the insets of Fig. 2 clearly show that both types of capacitor have the same grain size of 50 nm, though they exhibit a totally different $P-V$ curve. Tybell *et al.* identified a ferroelectric ground state even in 4 nm thick perovskite oxide films.[13] Junquera and Ghossez also reported that $BaTiO_3$ thin films between two metallic $SrRuO_3$ electrodes in a short circuit lost their ferroelectric properties below a critical thickness of about six unit cells (up to 2.4 nm).[14] We believe, therefore, that the collapse of the hysteresis loop in Fig. 2(b) is not due to the decrease of grain size caused by thickness reduction. High surface fields caused by heavy doping are another factor that degrades polarization; these fields can hide the microscopic ferroelectric switching polarization.[15] However, in this study, the chemical composition analysis by WDS did not reveal any impurities, which would likely affect the switching polarization.

The full width at half maximum (FWHM) of the (001) diffraction peak of the $BaTiO_3$ film on LSCO and the Pt electrode was determined to be 0.30° and 0.36° from Fig. 1, respectively. All $BaTiO_3$ films on both electrodes have nearly the same crystallinity. It was reported that $BaTiO_3$ heterostructure with ~0.38° of FWHM showed ferroelecrtric behavior with a small remnant polarization.[16] Therefore, the different behavior of Figs. 2(a) and 2(b) appears not to be due to the different crystallinity of the two capacitor stack. Furthermore, over the whole range of x-ray measurements from 20° to 60° on the $BaTiO_3/Pt$ stack, no other diffraction peaks related to any pyrochlore or second phase were observed.

The ferroelectricity in the epitaxial $BaTiO_3$ thin film is greatly affected by the biaxial in-plane stress.[17] The (002) peak in Fig. 1(a) clearly shifted to a high angle ($2\theta=46.17°$) compared to that of the $BaTiO_3$ single crystal ($2\theta_{(002)}=44.86$ Å, $2\theta_{(200)}=45.377$ Å),[18] indicating that the in-plane tensile stress is sustained in the film. The in-plane tensile stress could have an influence on the remnant polarization of the (001)-preferred orientation, but not on that of (100)-preferred orientation, because its polarization direction is perpendicular to an external field in the present capacitor structure. Thus, in this study, it appears that the low remnant polarization of the $Pt/BaTiO_3/LSCO$ capacitor in Fig. 2(a) is related to the decreasing of the c/a ratio of the (001)-preferred orientation (/or in the mixed structure) due to an in-plane tensile stress.[18] It is believed that if the in-plane tensile stress of $BaTiO_3$ on LSCO electrode relaxes, the remanent polarization will be enhanced because of an increasing of c/a ratio.[17] On the other hand, the $BaTiO_3$ films on the Pt electrode in Fig. 1(b) lie under a nearly free stress state because the diffraction peak positions of the film were in accord with those of bulk $BaTiO_3$.[19] Therefore, we believe that the disappearance of ferroelectricity in the $Pt/BaTiO_3/Pt$ capacitor in Fig. 2(b) is not due to the stress effect in the film.

The remanent polarization of $BaTiO_3$ film is also dependent on the film texture.[20,21] Tada *et al.*[20] reported that an {111} epitaxial $BaTiO_3$ film grown on a {111} Pt substrate has a smaller P_r compared to a totally random oriented polycrystalline $BaTiO_3$ film. However, Yang *et al.*[21] reported that, on a $LSCO/Pb(Nb_{0.04}Zr_{0.28}Ti_{0.68})O_3/LSCO$ capacitor, polycrystalline materials show a lower remanent polarization than epitaxial material. Considering the previous study, the random oriented polycrystalline $BaTiO_3$ film or the highly (111) oriented $BaTiO_3$ film does not lose its remanent polarization completely. Therefore, the effect of texture structure on the linear dielectric property of $BaTiO_3/Pt$ stack in this study could be inconsiderable. To elucidate the cause of the different behavior in the hysteresis loops for the capacitors with a $Pt/BaTiO_3/Pt$ and $Pt/BaTiO_3/LSCO$ structure of 100 nm film thickness, the cross-sectional high-resolution microstructures were investigated using TEM.

From the cross-sectional HRTEM image in Fig. 3(a), it is clear that there is no any interfacial layer between $BaTiO_3$ and LSCO electrode. However, the HRTEM image of Fig. 3(b) clearly reveals that the disturbed interfacial layer was formed at the interface between the $BaTiO_3$ film and the Pt bottom electrode. The insert of Fig. 3(b) shows the distinct multidomain structure in the interior of each columnar grain with a width of 40–50 nm. This multidomain structure clearly reflects the existence of ferroelectricity in the $BaTiO_3$ film grown on a Pt electrode, although the $Pt/BaTiO_3/Pt$ capacitor exhibits a linear dielectric property from polarization versus applied voltage. Therefore, the experimental re-

Downloaded 18 Apr 2011 to 143.248.103.56. Redistribution subject to AIP license or copyright; see http://apl.aip.org/about/rights_and_permissions

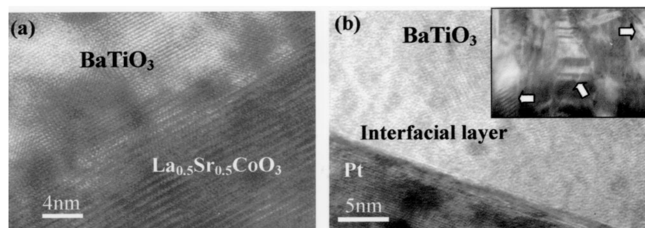

FIG. 3. Cross-sectional HRTEM images of $BaTiO_3$ films grown on (a) $La_{0.5}Sr_{0.5}CoO_3$ and (b) Pt bottom electrodes. The inset (b) is a cross-sectional TEM image indicating the existence of a multidomain structure in the interior of $BaTiO_3$ film grown on the Pt bottom electrode.

sult shown in Fig. 3(b) strongly suggests that the disappearance of ferroelectricity in the $Pt/BaTiO_3/Pt$ capacitor was caused by the formation of the interfacial layer between the $BaTiO_3$ thin film and the bottom electrode. As Vendik *et al.* pointed out,[3] the ferroelectric polarization of a film in contact with conducting oxides can penetrate the electrodes. Consequently, the interfacial layer, but not the Pt electrode, is eliminated; furthermore, the penetration of the polarization is not feasible due to the high free electron density and the nonpolarizing nature of Pt. This process therefore results in the creation of the disturbed interfacial layer. Moreover, as elucidated by Vendik *et al.*, this layer is classified as having an "intrinsic origin" because it simply originates from the absence of dielectric materials from the surface or electrode film; and this phenomenon is used to explain the thickness dependence of the dielectric constant.[2,4] The interfacial layer shown in Fig. 3(b), however, has an amorphous structure that is not clearly related to an intrinsic origin.

Figure 4 shows a linear relationship between d_m/ε_m and the total film thickness. According to Eq. (1), the linear slope indicates $1/\varepsilon_f$, while the y axis intercept is d_i/ε_i. Considering that the thickness of the interfacial layer d_i is 5 nm, as shown in Fig. 3(b), we extract an interfacial dielectric constant ε_i, of 26, which agrees well with the measured dielectric constant of amorphous $BaTiO_3$ film reported by Thomas *et al.*[22] Therefore, in this study, we suggest that the degradation of polarization in the $BaTiO_3/Pt$ capacitor might have originated from the formation of the interfacial layer and

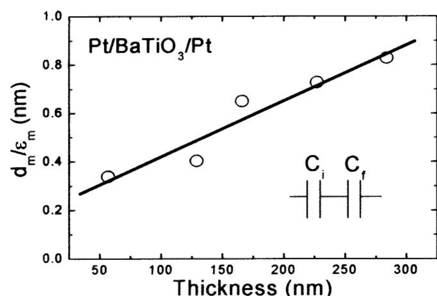

FIG. 4. Experimental plot of d_m/ε_m vs the total thickness of the $BaTiO_3$ film grown on Pt. The solid line is the best linear fit to the data. The best fit indicates that the interfacial layer between the $BaTiO_3$ film and the Pt bottom electrode has a dielectric constant of 26.

also, this layer's origin can be categorized as extrinsic because it is generated by the disorder of the crystallographic structure. It is considered that this disordered interfacial layer is likely to form at the interface between the film and the bottom electrode because of the interfacial diffusion of Pt/Ti into the ferroelectric film.

In summary, we obtained different features of polarization in two types of $BaTiO_3$ capacitors that, respectively, used LSCO and Pt as bottom electrodes. While the $Pt/BaTiO_3/LSCO$ capacitor showed a well-saturated hysteresis loop, collapse of the remnant polarization P_r in the $Pt/BaTiO_3/Pt$ capacitor was observed in the $P-V$ curve although the $Pt/BaTiO_3/Pt$ structure showed a multidomain structure in the interior of the $BaTiO_3$ film. The polarization degradation in the $BaTiO_3/Pt$ structure is attributed to the existence of an extrinsic interfacial layer with an amorphous structure formed between the ferroelectric film and the Pt bottom electrode.

This work was supported by the Ministry of Science and Technology Grant No. M1010500066-01H2006400, the National Research Laboratory Program Grant No. M10400000024-04J0000-02410, and the Brain Korea 21 Project in 2004.

[1] B. T. Lee and C. S. Hwang, Appl. Phys. Lett. **77**, 124 (2000).
[2] S. K. Streiffer, C. Basceri, C. B. Parker, S. E. Lash, and A. I. Kingon, J. Appl. Phys. **86**, 4565 (1999).
[3] O. G. Vendik, S. P. Zubko, and L. T. Ter-Martirosayn, Appl. Phys. Lett. **73**, 37 (1998).
[4] C. Zhou and D. M. Newns, J. Appl. Phys. **82**, 3081 (1997).
[5] P. K. Larsen, G. J. M. Dormans, D. J. Taylor, and P. J. van Veldhoven, J. Appl. Phys. **76**, 2405 (1994).
[6] J. C. Shin, J. H. Park, C. S. Hwang, and H. J. Kim, J. Appl. Phys. **86**, 506 (1999).
[7] J. J. Lee, C. L. Thio, and S. B. Desu, J. Appl. Phys. **78**, 5073 (1995).
[8] K. V. Im, B. J. Kuh, S. O. Park, S. I. Lee, and W. K. Choo, Jpn. J. Appl. Phys., Part 1 **39**, 5437 (2000).
[9] C. V. Thompson, J. Appl. Phys. **58**, 763 (1985).
[10] H. J. Frost and C. V. Thompson, Acta Metall. **35**, 529 (1987).
[11] J. W. Jang, S. J. Chung, W. J. Cho, T. S. Hahn, and S. S. Choi, J. Appl. Phys. **81**, 6322 (1997).
[12] Y. Sakashita, H. Segawa, K. Tominaga, and M. Okada, J. Appl. Phys. **73**, 7857 (1993).
[13] T. Tybell, C. H. Ahn, and J. M. Triscone, Appl. Phys. Lett. **75**, 856 (1999).
[14] J. Junquera and P. Ghosez, Nature (London) **422**, 506 (2003).
[15] F. K. Chai, J. R. Brews, and R. D. Schrimpf, J. Appl. Phys. **78**, 4766 (1995).
[16] C. Schwan, J. C. Martin, and H. Adrian, Proceedings of EUCAS 1997 Third Europan Conference on Applied Superconductivity (1997), p. 805.
[17] K. J. Choi, M. Biegalski, Y. L. Li, A. Sharan, J. Schubert, R. Uecker, P. Reiche, Y. B. Chen, X. Q. Pan, V. Gopalan, L-Q. Chen, D. G. Schlom, and C. B. Eom, Science **306**, 1005 (2004).
[18] H. Miyazawa, E. Natori, T. Shimoda, H. Kishimoto, F. Ishii, and T. Oguchi, Jpn. J. Appl. Phys., Part 1 **40**, 5809 (2001).
[19] H. E. Swanson and R. K. Fuyat, Natl. Bur. Stand. Circ. (U. S.) **3**, 45 (1954).
[20] O. Tada, Y. Shintani, and Y. Yoshida, J. Appl. Phys. **40**, 498 (1969).
[21] B. Yang, S. Aggarwal, A. M. Dhote, T. K. Song, R. Ramesh, and J. S. Lee, Appl. Phys. Lett. **71**, 356 (1997).
[22] R. Thomas, D. C. Dube, M. N. Kamalasanan, and N. D. Kumar, J. Sol-Gel Sci. Technol. **16**, 101 (1999).

Downloaded 18 Apr 2011 to 143.248.103.56. Redistribution subject to AIP license or copyright; see http://apl.aip.org/about/rights_and_permissions